Article

The Design of High Efficiency Crossflow Hydro Turbines: A Review and Extension

Ram Adhikari [†] and David Wood *,[†] (ID)

Department of Mechanical and Manufacturing Engineering, University of Calgary, 2500 University Drive NW, Calgary, AB T2N 1N4, Canada; rcadhika@ucalgary.ca

* Correspondence: dhwood@ucalgary.ca; Tel.: +1-403-220-3637

† These authors contributed equally to this work.

Abstract: Efficiency is a critical consideration in the design of hydro turbines. The crossflow turbine is the cheapest and easiest hydro turbine to manufacture and so is commonly used in remote power systems for developing countries. A longstanding problem for practical crossflow turbines is their lower maximum efficiency compared to their more advanced counterparts, such as Pelton and Francis turbines. This paper reviews the experimental and computational studies relevant to the design of high efficiency crossflow turbines. We concentrate on the studies that have contributed to designs with efficiencies in the range of 88–90%. Many recent studies have been conducted on turbines of low maximum efficiency, which we believe is due to misunderstanding of design principles for achieving high efficiencies. We synthesize the key results of experimental and computational fluid dynamics studies to highlight the key fundamental design principles for achieving efficiencies of about 90%, as well as future research and development areas to further improve the maximum efficiency. The main finding of this review is that the total conversion of head into kinetic energy in the nozzle and the matching of nozzle and runner designs are the two main design requirements for the design of high efficiency turbines.

Keywords: crossflow hydro-turbine; maximum efficiency; flow features; RANS simulation

---

1. Introduction

The turbine is the core component of hydropower systems and improving its efficiency, defined as the ratio of power extracted from the water to the product of the mass flow rate, gravity, and available head at the turbine. This definition is used in most, but not all, previous studies. Efficiency has a clear link to increased power output and reduced system cost. The crossflow turbine is simpler in design and cheaper to manufacture than other types such as Pelton, Turgo, and Francis. Crossflow turbines are mostly used in remote power systems in developing countries, and have a typical efficiency in the range of 70–85%. Despite the efficiency being lower than other types, the crossflow turbine exhibits a flatter efficiency curve with varying runner angular velocity, ω, which can be an important advantage. Since its invention by Michell in 1903 [1], the key design problem has been to improve its maximum efficiency, η_{max}. This review highlights the most important design features and key design principles for achieving efficiencies of around 90%. Our emphasis is on synthesizing the results of the most efficient turbine designs, in order to provide a basis for future designs.

As shown in Figure 1, the crossflow turbine comprises two main components: a stationary nozzle and a rotating runner. The nozzle accelerates the inlet flow and directs it at the runner at angle β_1. For maximum efficiency, β_1 should match the outer blade angle of the runner taking into account the transfer from stationary to rotating co-ordinates. The latter angle is omitted from Figure 1 for clarity. Nozzle design is important because the runner entry flow directly affects the performance of the runner, which, in turn, must be designed to extract the maximum amount of angular momentum (Adhikari

and Wood [2]). In this review, we do not consider a guide vane as used in most actual turbines for controlling the inlet flow. In Figure 1, a guide vane would normally be upstream of the nozzle throat; for details, refer to Figure 7 of Paish [3]. A guide vane significantly reduces the quality of the inlet flow by splitting it into two jets and producing non-uniform entry flow angles that can cause a serious loss in turbine efficiency. Adhikari and Wood [2] showed that flow control is required to maintain high efficiency at part load, that is, unchanged H at reduced Q, so an alternative to a guide vane is required. A good choice appears to be the slider at the runner entry described by Sinagara et al. [4]. The slider is a circular segment that reduces the entry arc length, θ_s in Figure 1, as the Q decreases. Adhikari [5] showed computationally that this flow control mechanism does not reduce η_{max} at design flow rates and can also maintain part-load efficiency close to the maximum. As maximum efficiency at full load is the topic of this review, we omit consideration of the part-flow control mechanism.

Adhikari and Wood [2] presented a methodology for designing nozzles without a vane based on conversion H at the nozzle inlet into kinetic energy at entry to the runner, which is the same principle that governs Pelton nozzle design. Assuming that W, the width out of the page in Figure 1, is the same for the nozzle and runner; this principle leads to straightforward equations for the nozzle rear-wall, given by their Equation (5) for tangential entry (angle $\delta = 0$ in in Figure 1) and their (7) for the more general oblique entry ($\delta > 0$) shown in the figure.

Figure 1. Schematic illustration of key geometrical parameters of crossflow turbine [2].

The key geometrical parameters for the runner are the inner to outer radius ratio (R_2/R_1), outer blade angle (β_{1b}), inner blade angle (β_{2b}), and number of blades (N_b). Of these, β_{1b} must be close to β_1 to avoid separation on the blades and loss of efficiency, leaving only R_2/R_1 and N_b as parameters to be varied in seeking maximum efficiency. The circular arc blades usually have small thickness. Figure 1 shows a unique feature of the crossflow turbine; the flow passes twice through the rotating runner. The flow enters from the nozzle, passes through the "first stage", traverses the central air-space, and exits through the "second stage". Often, the first stage does not convert all the available energy into power, Choi et al. [6]. This dual use of the blades to extract power requires a change to conventional blade terminology: we use "outer" and "inner" for the blade angles in either stage. In addition, "inlet" describes the flow anywhere in the nozzle with "entry" referring specifically to the flow as it passes

from the inlet to the runner. For maximum performance, at the runner angular velocity ω, β_1 is easily found to be

$$\beta_1 = tan^{-1}\left(\frac{u_r}{u_\theta - \omega R_1}\right), \tag{1}$$

where subscript "r" indicates a radial, and "θ" a tangential component, and it is assumed that the runner entry velocities are uniform. This is Equation (10) of Adhikari and Wood [2]. By matching kinetic energy at the runner entry to the product of runner torque and ω, and assuming that *no angular momentum exits the second stage*, Equation (14) of Adhikari and Wood [2] gives the optimum ω, ω_{max}, for nozzle velocity U_0 according to

$$\omega_{max}R_1 = \frac{U_0}{2}\left(1 + \frac{h_0^2}{R_1^2\theta_s^2}\right). \tag{2}$$

Note that the runner parameters are on the left side of Equation (2) and the nozzle parameters on the right side. R_1 is common to the nozzle and runner. Note further that the second term on the right, $h_0^2/(R_1^2\theta_s^2)$, is usually much less than unity, so this criterion for optimum performance is close to that for a Pelton turbine, which is not surprising as the design principle for the nozzle of both turbine types is the same.

We divide the previous studies of crossflow turbines by whether they were mainly experimental or numerical. There are also some analytic formulations for calculating turbine efficiency (e.g., Mackmore and Merryfield [7]), but Adhikari [5] showed they are not accurate, and are thus omitted from this review. Most experimental studies were of the effects on turbine performance of varying the runner geometry without measuring the internal flow and its impact on efficiency. Thus, the only measurement available is the turbine efficiency as a function of ω as a function of H and Q. Similarly, most numerical studies focused on performance prediction of individual turbines using Reynolds-average Navier–Stokes (RANS) simulations, rather than on the study of internal flow that is important for improving the maximum efficiency. Only recently, Adhikari [5] characterized the main flow features of 8–90% efficient turbines, and applied these to improve the efficiency of a turbine measured at 67–91%. We anticipate that these results provide fundamental design principles for further improvement of η_{max}. Therefore, we concentrate on high efficiency turbines. None of these turbines with high η_{max} had a guide vane.

The structure of this paper is as follows. The next section reviews the experimental work. Then, Section 3 does the same for the computational studies, emphasizing the flow features and possibilities for design improvements. The main design principles are collected in Section 4, which is followed by a list of areas for future work and the main conclusions.

2. Experimental Studies

The main geometrical features of turbine design are well known, but their combined effects on performance are not. The important previous studies [7–20] are listed in chronological order and summarized in Table 1. Most have reported $\eta_{max} \approx 82\%$ or less, which is significantly lower than that the typical maximum efficiency for the Pelton, Francis and Kaplan turbines of over 90%. Only three experimental studies have reported η_{max} in the range 88–90% and *none* of these used a guide vane in the nozzle. Fiuzat and Akerkar [18] found $\eta_{max} \approx 90\%$ at part-flow conditions with a flow diverter in the air-space but did not achieve maximum efficiency at the design flow. Desai [19] developed a 0.53 kW turbine with $\eta_{max} = 88\%$ from extensive testing of various designs. In continuation of his work, Totapilly and Aziz [20] achieved a remarkable $\eta_{max} = 90\%$ just by increasing the number of blades from 30 to 35. These turbines are the most efficient crossflow turbines reported in the literature; no larger-scale turbines of comparable efficiency have been reported. Unfortunately, no measurements have been made of the nozzle flow or that in the two stages of the runner, which should be valuable in guiding the design of more efficient turbines. Recently, Adhikari [5] used the experimental results

of Desai [19] and Totapally and Aziz [20] in a computational study to understand the dominant flow features. The major findings will be presented in the next section.

Table 1. Summary of the design parameters used in the experimental studies. * indicates a value for maximum efficiency. Symbols are defined in Figure 1.

Source	δ	β_{1b}	β_{2b}	R_2/R_1	N_b	θ_s	η
	(deg)	(deg)	(deg)	(-)	(-)	(deg)	(%)
Macmore and Merryfield [7]	16	30	90	0.66	20	-	68
Varga [8]	16	39	-	0.66	30	-	77
Durali [9]	16	30	90	0.68	24	-	76
Dakers and Martin [10]	22	30	90	0.67	20	69	69
Johnson and White [11]	16	39	-	0.68	18	60	80
Nakase et al. [12]	15	39	-	0.68	26	90	82
Durgin and Fay [13]	16	39	-	0.68	20	63	66
Khosrowpanah [14,15]	16	39	90	0.68	15	58, 78, 90 *	80
Horthsall [16]	16	-	-	0.66	21	-	75
Ott and Chappell [17]	16	-	-	0.68	20	-	79
Fiuzat and Akerker [18]	20–24 *	39	90	0.68	20	90	89
Desai [19]	22 *–32	39	90	0.60–0.68 *–0.75	30	90	88
Totapally and Aziz [20]	22 *–24	39	55 *–90	0.68	35	90	90

The influence of the nozzle inclination, δ in Figure 1, on the efficiency was studied by [12,14,18–20] and others. It has been assumed that $\delta = \tan^{-1}(u_r/u_\theta)$, where u_r is the radial velocity and u_θ is the tangential velocity at the entry to the runner. Khosrowpanh [14] and Nakase et al. [12] found that $\delta = 16°$ gave the maximum efficiency between 80% and 82%. Fiuzat and Akerker [18] found that $\eta_{max} = 89\%$ at $\delta = 24°$, and Desai [19] reported the $\eta_{max} = 88\%$ at $\delta = 22°$. Similarly, Totapally and Aziz [20] found $\eta_{max} = 90\%$ at $\delta = 22°$. It is emphasized, however, that matching of β_1 and β_{1b} is more relevant than δ in avoiding the flow separation on the blades. Furthermore, the nozzle design methodology of Adhikari and Wood [2] includes the effect of δ directly and determines u_r mainly from the θ—dependence of the rear-wall shape, $R(\theta)$. The influence of β_{1b} and β_{2b} has been studied by several researchers [19,20]. These angles affect flow separation on the blades, the runner efficiency, and the relative power output of the first and second stages. The majority of previous studies found η_{max} occurred at $\beta_{1b} = 39°$, whereas β_{2b} was kept at 90°. Desai [19] found that $\beta_{2b} = 90°$ gave the maximum efficiency, whereas Totapally and Aziz [20] found that $\beta_{2b} = 55°$ gave slightly greater maximum efficiency than $\beta_{2b} = 90°$. It is noted that the nozzle design greatly influences the magnitude and uniformity of β_1 at the runner entry, which should match β_{1b}.

The impact of the nozzle rear-wall shape, $R(\theta)$ in Figure 1, was studied by Nakase et al. [12]. Circular and logarithmic spiral shapes gave nearly the same peak efficiency. However, they did not investigate the effect of $R(\theta)$ on the runner performance. Nozzle design was also studied by Dakers and Martin [10] for a 7 kW turbine with $\beta_{1b} = 30°$, $\beta_{2b} = 90°$, $R_2/R_1 = 0.68$ and $N_b = 20$ for $H = 10$ m and $Q = 105$ lps. By changing the rear wall shape and orientation, they achieved $\eta_{max} = 69\%$ for the same runner. Extensive measurements were done at varying H, Q, and N_b. Their work also includes detailed information of the turbine geometry, the operating conditions, and results in allowing meshing for a computational simulation. This turbine has been numerically investigated by Adhikari [5] and Adhikari et al. [21] for cavitation, and by Adhikari [5] and Adhikari and Wood [2] for performance losses and design improvement. The results will be reviewed in the next section.

Refs. [12,14,18] and others investigated the influence of nozzle entry arc angle, θ_s, on the efficiency. They found that $\theta_s = 90°$ gave the maximum efficiency. Fiuzat and Akerkar [18] and Totapally and Aziz [20] found that vertically oriented nozzles with $\theta_s = 90°$ had $\eta_{max} \approx 90\%$. However, they did not compare the efficiency difference between horizontal and vertical orientations. We believe the differences would be marginal as is the case for Pelton turbines. The relevant non-dimensional

parameter from Equation (2) is $h_0/(R_1\theta_s)$. We show later that this parameter has the value 0.34 for a low efficiency turbine (69%) and 0.37 for high efficiency turbines (88–90%), so there is not much difference.

Studies on the influence of R_2/R_1, which do not appear directly in Equation (1) or (2), on the efficiency have determined that the value 0.68 is optimum [7,9,10,12,14,15,18–20]. Smaller R_2/R_1 means longer blades and reduces the size of the central air-space of the runner, where the water streams exiting the multiple blade passages of the first stage combine before passing through the second stage. The influence of R_2/R_1 on the internal flow structure and the runner performance has not been studied.

The influence of N_b on η_{max} also cannot be guided by theory; Equations (1) and (2), and the principle of conversion of H to entry kinetic energy, do *not* depend on N_b. It is likely that, starting from a small value, increasing N_b will increase η_{max} until the point at which boundary layer blockage becomes important, after which η_{max} decreases. The influence of N_b on efficiency was studied by [12,14,19,20] by varying N_b. Khosrowpanh [14] conducted experiments with N_b = 10, 15 and 20; fifteen blades gave the highest $\eta_{max} \approx 80\%$. Nakase [12] found that N_b = 26 is the optimum N_b for a runner with R_1 = 157.5 mm. Desai [19] and Totapally and Aziz [20] found that $N_b = 30$ and 35 gave $\eta_{max} = 88\%$ and 90% respectively. However, Fiuzat and Akerker [18] obtained $\eta_{max} = 89\%$ with 20 blades on a similar size runner to that used by Desai [19] and Totapally and Aziz [20]. As mentioned above, no measurements of the flow in the runner have ever been made so the effect of N_b on flow separation on the blades and, therefore, efficiency cannot be deduced experimentally.

Simple nozzle design theory does not allow assessment of the stage contributions to the total power by controlling the geometric parameters β_{2b} and N_b. It is not surprising that there are no measurements of the division of the total power between the first and second stages. Fiuzat and Akerkar [22] designed a special turbine with a flow diverter in the internal air-space to measure the relative contributions of the two stages to the total power output. A significant percentage of the power was extracted at the second stage; at least 45% for $\theta_s = 90°$, and at least 41% for $\theta_s = 120°$. They argued that turbine efficiency can be improved by increasing the crossflow in the air-space, which will increase the output from both stages. The applicability of this result is limited because they did not study the influence of β_{1b}, β_{2b} and N_b on stage performance. The computational determination of relative stage performance in the next section suggests that second stage extraction can be significant at η_{max}.

No experiment considered the internal flow characteristics and their effect on turbine efficiency. Durgin and Fay [13] visualized the internal flow with an open-ended, cantilevered runner. They placed an external flow deflector inside the runner to control the flow direction and measure the contributions of each stage. They varied θ_s and measured Q and the flow "trapped" in the blade passages after the first stage and prevented from entering the second stage. It is noted that the trapped flow does not pass through the central air-space. The flow passing through the central region was called "crossflow" and the appellation "crossflow turbine" appears for the first time in the work of Durali [9]. Durgin and Fay [13], however, could perform the experiments only at part-load, but not at design Q due to high flow interaction. The most significant result was the amount of trapped flow inside the blade passages. It was directed tangentially, and increased as the speed increased or as the crossflow decreased. In addition, as θ_s was increased from 30 to 80°, the amount of trapped flow increased. They obtained $\eta_{max} = 61\%$ and found the second stage contributed only 17% to the total power production. However, their findings were not generalized, and are of limited help in achieving efficiencies of 88–90% or higher. Nevertheless, the split between the stages is interesting, particularly because this is the only measurement apart from Fiuzat and Akerker [22], and it suggests that the crossflow design inherently allows "recovery" in the sense that power not extracted by the first stage may be extracted in the second. They also observed that a significant amount of trapped flow did not lead to power extraction at the second stage. In one of the early theoretical analyses, the runner flow was assumed to move through the central region of the runner as an ideal, "well-developed single jet" [7]. Durgin and Fay [13] did not observe this regime as the only one in their experiment.

They also concluded that the trapped flow varied with ω and caused significant incidence losses at the second stage. θ_s impacted the amount of flow passing through the central air-space, and the efficiency improved as the amount of crossflow increased. They modified the turbine for the effects of trapped flow, which slightly improved the η_{max} to 66%. Their observations, however, are not likely to be useful in achieving efficiencies around 90%.

3. Computational Studies

Although the key geometril features and their effects on turbine efficiency have been experimentally studied, this knowledge does not readily help to design high efficiency turbines, partly because of the lack of knowledge about the details of the runner flow. As it is difficult and expensive to measure and visualize the flow fields in the runner, the alternative is computational simulations. Because the studies under review modeled the whole turbine, it seems better to review them chronologically, rather than by specific feature, as was done in the previous Section. Recent RANS simulations include [4,6,23–26]; however, they provide little of the flow, and do not address the design problem of improving efficiency. These studies have employed the k-ϵ and shear stress transport (SST) k-ω turbulence models with homogeneous, two-phase free-surface models for water and air. Most studies investigated low-efficiency turbines and were aimed at predicting the turbine performance. Moreover, the reported flow patterns were only basic, rather than a detailed identification of the loss mechanisms and their influence on the runner performance. Typically, η can be determined to within 6% and there is little difference between the two turbulence models referred to above, e.g., [2]. Typical results from [2] are shown in Figure 2; in addition, it is clear that unsteady RANS (URANS) models do not seem to provide increased accuracy.
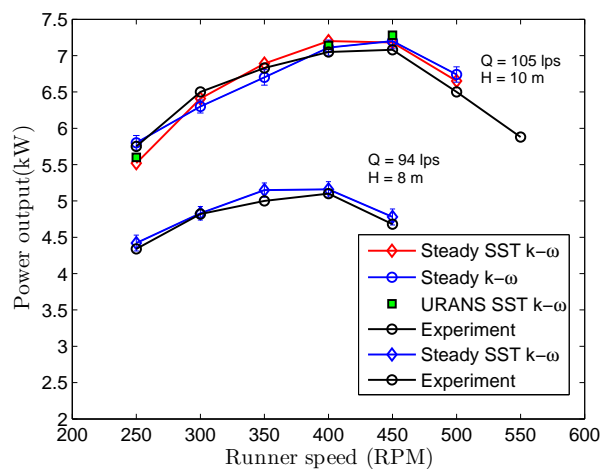
Figure 2. Comparison of CFD and experimental results for the power output of the 7 kW turbine at different flow rates and heads.

The key nozzle design principle: the need for conversion of head into kinetic energy at the runner entry, formulated by [2], was not considered previously, and little information is available in prior studies on the role of the entry velocities u_θ and u_r, or β_1 on the runner performance and turbine efficiency.

Choi et al. [6] showed that guide vane setting in the nozzle influences efficiency during part-flow operations, possibly due to improving the nozzle flow and maintaining a suitable angle of attack. The improvement, however, is relative to $\eta_{max} \approx 80\%$. Apart from Acharya et al. [25], discussed below, this is the only computational study to include a guide vane, but, unfortunately, no details were provided of the nozzle flow and the effect of the guide vane on it. They also showed that an air-layer in the blade passages, via suction through air vents around the runner, improved efficiency by reducing recirculation in the blade passages.

De Andrade et al. [23] used 3D steady RANS computations with a water–air homogeneous flow model, free-surface effects, and the k-ϵ turbulence model. They found that about 68% of the power is produced in the first stage in a turbine with $\eta_{max} \approx 70\%$. They determined β_1 and β_2 and the angle at the inlet of the second stage. A significant difference was found between β_1 and β_{1b}. However, no attempt was made to use this information for design improvement.

Sammartano et al. [24] describe a two-step design methodology for the optimal design of crossflow turbines but defined efficiency in terms of the head difference between inlet and outlet. This gives a higher value than the definition used here. The first step is a simple analytical nozzle design equation. The second gives a set of empirical values for the runner design, which can be refined using steady and unsteady RANS computations. A simulation of a 5.2 kW turbine of optimal design, using steady and unsteady RANS computations and the SST k-ω turbulence model and two-phase homogeneous model with free-surface effects, gave a maximum efficiency of 86%. However, this efficiency must be greater than the more common one used here. As discussed in the previous section, η_{max} in the range of 88–90% has already been achieved by [18–20] and thus [24] does not indicate the most desirable design attributes of high efficiency turbines. More importantly, they did not provide a fundamental analysis of the flow characteristics and loss mechanisms, and their influence on the runner performance.

Acharya et al. [25] performed steady RANS computations on a turbine with $\eta_{max} = 63\%$. They used the SST k-ω turbulence model with the homogeneous multiphase model for modeling water and air with free-surface effects. They modified the nozzle rear wall of circular shape, adjusted the guide vane opening, and changed N_b from the reference turbine. This increased η_{max} from 63 to 76%. However, they did not document the changes in the flow field, and the effects on the runner performance. Specifically, no detailed analysis was attempted for the nozzle and guide vane performance, inlet flow conditions, and power extraction in the two stages. Therefore, the results are of limited use for design improvement. Following the same design procedure presented in reference [24], Sammartano et al. [26] designed and evaluated corssflow turbine performance using RANS simulations and measurements. However, their design gave $\eta_{max} = 80.6\%$ and so their work is not considered further.

In a recent computational study, Adhikari et al. [21] showed that cavitation can occur in crossflow turbines. Using steady RANS computations with the SST k-ω turbulence model and homogeneous multiphase model for water and air with free-surface effects, they studied cavitation inception on the 7 kW turbine of [10]. Cavitation started at the inner edges of the second stage blades at and above ω_{max}. This study suggests that cavitation may be an important consideration for crossflow turbines but only if they are poorly designed to operate past the maximum efficiency point in terms of Q. No further information about cavitation in crossflow turbines is available in the literature. Further experimental and numerical investigations are needed to test the generality of the specific conclusion reached from numerically studying one turbine with low efficiency.

Adhikari [5] characterized the key flow features of low and high efficiency turbines. The 7 kW turbine with $\eta_{max} = 69\%$ of [10] showed massive flow separation on the blades, shown in Figure 3, caused by a significant difference between β_1 and β_{1b}. In addition, the inlet H was not converted into kinetic energy in the nozzle [2]. The schematic of the turbine geometry is shown in Figure 4 and the geometrical parameters are presented in Table 2.
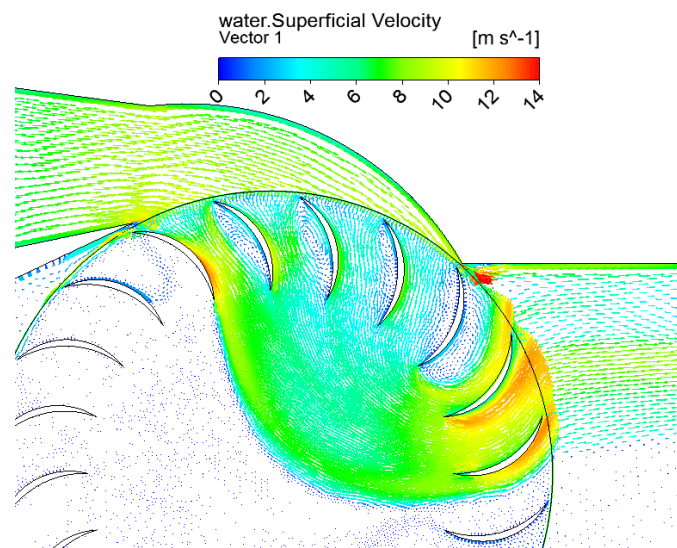
Figure 3. Water velocity vectors illustrating the flow separation on the blades at the first stage of the 7 kW turbine at $\eta_{max} = 69\%$. Note that there is no flow separation on the second stage [5].
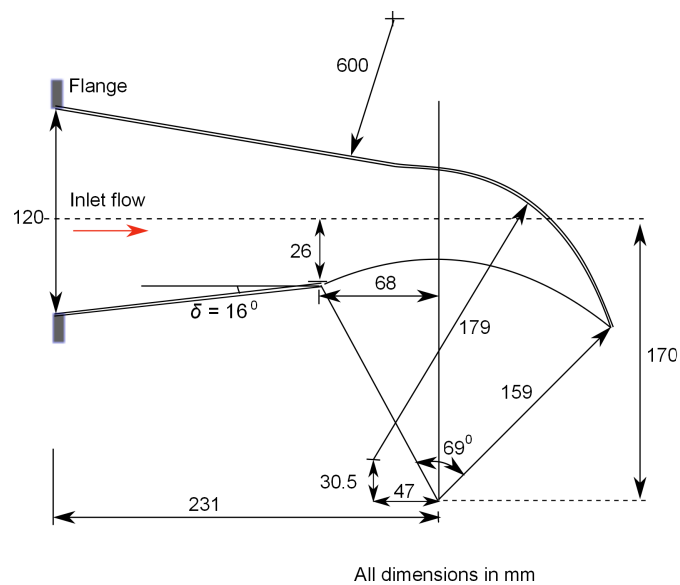

All dimensions in mm

Figure 4. Schematic illustration of the 7 kW turbine [10] with $\eta_{max} = 69\%$. The three lines converge at the runner axis [5].

By matching of nozzle and runner designs using $\beta_1 \approx \beta_{1b}$, Desai [19] achieved a high efficiency. Here, we describe only the main results relevant to numerical simulation. A schematic diagram of his high efficiency turbine is shown in Figure 5 and the geometric parameters are listed in Table 2. Measurements were performed at different flow rates and heads and speeds. The main geometrical parameters varied were β_{1b}, β_{2b}, N_b, R_2/R_1, δ, and θ_s.
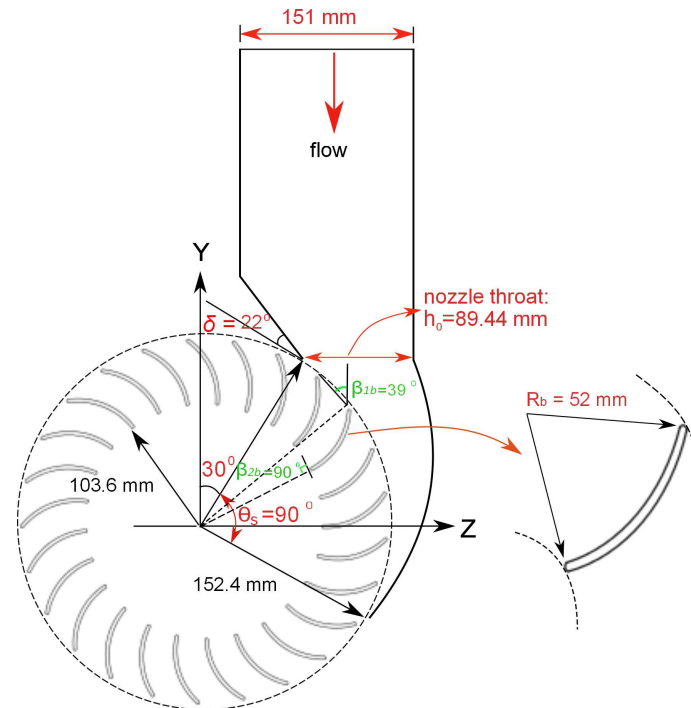
Figure 5. Schematic illustration of the 0.53 kW turbine [19] with $\eta_{max} = 88\%$ [5].

Table 2. Design parameters of 7 kW and 0.53 kW [19] turbines studied by [2] and [5]. β_1 is evaluated at ω_{max} from Equation (2).

Design Parameter	7 kW Turbine	0.53 kW Turbine	Improved 7 kW Turbine	Improved 0.53 kW Turbine
Outer radius (R_1), (mm)	158	152.4	158	152.4
Inner radius (R_2), (mm)	105.86	103.63	105.86	103.63
Outer blade angle (β_{1b}), (°)	30	39	39	39
Inner blade angle (β_{2b}), (°)	90	90	90	90
Blade thickness (t), (mm)	3	3.2	3	3.2
Number of blades (N_b)	20	30	35	35
Runner and nozzle width (W), (mm)	150	101.6	94.34	101.6
Nozzle throat (h_0), (mm)	65	89	83	89
Nozzle entry arc (θ_s), (°)	69	90	80	90
η_{max}, (%)	69	88	91	90
ω_{max}, (RPM) (Exp, CFD)	450	199.1	500	199.1
ω_{max} from Equation (2), (RPM)	363	183	461	183
β_1 from Equation (1), (°)	37.7	41	41	41
$h_0/(R_1\theta_s)$	0.34	0.37	0.37	0.37

In the following sections, we review the main results of computational studies of [5] to which the reader is referred for more details.

3.1. The Flow in Crossflow Turbines

We will continue to treat the runner blades as thin circular arcs because this is essential for reducing the cost and ease of manufacture of crossflow turbines. With this assumption, the main runner parameters that are not fixed by the nozzle—see Equations (1) and (2)—are N_b, β_{2b}, and R_2/R_1 or R_2. The values of these parameters for the two turbines under consideration are given in Table 1 of [2], which is reproduced here also as Table 2 for convenience. Figures 4 and 5, also given in [2], provide the remaining information on the geometry.

The performance of the 7 kW turbine is shown in Figure 2. Figure 3, which is Figure 11 of [2], shows the computed flow through the 7 kW turbine at η_{max} and ω_{max} = 450 RPM. It is clear that there is significant flow separation from the blades in the first stage, but surprisingly not in the second stage. Figure 6a (Figure 14 of [2]) shows the corresponding flow for the 0.53 kW turbine indicating

no separation in the runner. (Part (b) of Figure 6 will be discussed below.). For both turbines, it is remarkable that the second stage is contiguous with the first. As ω increased, β_2 at the first stage increased, whereas the second stage inlet flow angle β_{2i} decreased. As a result, the flow was deflected more toward the upper region of the second stage. It is noted that as the exit area of the first stage is reduced by a factor of R_2/R_1 from the entry area, so the flow converges as it passes through the first stage. Thus, the area occupied by the water decreased as the runner speed increased. It is noteworthy (but not shown here for brevity) that, at low ω, the flow passed through more of the air-space and the angular extent of the two stages increased. The results are also consistent with the experimental observations of [13] and numerical simulations of [23]. At ω_{max}, β_{2i} closely matched the inner blade angle β_{2b}. The detailed analysis can be found in [5]. It is noteworthy that the flow entering the second stage is influenced by R_2/R_1. As the ratio increases, there is less of a chance of flow separation in the second stage than in the first stage even if β_{2i} differs from β_{2b}. However, it does not necessarily improve the power extraction or the efficiency; detailed studies of the influence of R_2/R_1 on efficiency and stage performance can be found in [5] where the value from Table 1, $R_2/R_1 = 0.68$ is confirmed. That the two stages can occupy less than $180°$ suggests the use of two opposing nozzles, much like a double jet Pelton turbine, which could double the power density, and reduce cost per unit power and sources of vibration.

Velocity vectors and contours give only a general view of the runner performance. In particular, they do not show the distribution of the power extraction around the runner. This is plotted for the 7 kW turbine in Figure 7 in terms of the power produced per blade, determined by using a control volume analysis for each blade's contribution to runner torque. The azimuthal angle ψ is measured relative to the horizontal, which is in the $-z$ direction in Figure 5. Thus ψ has a different origin to θ which is zero at the start of the first stage. There is a significant variation in power production between the blades in the first stage of the 7 kW turbine. The reason is that β_1 is significantly larger than β_{1b} near the nozzle throat (see Figure 10 of [2]). β_1 then decreases for the remaining blades but is always greater than β_{1b}. This causes the flow separation shown in Figure 3 and the poor power production in this stage. Similarly, there is a significant azimuthal variation in the second stage power production that has peaked over a small portion of that stage. This is due to the azimuthal variation in the flow angle β_{2i} at the entry of the second stage or the effect of increasing runner speed. At ω_{max} = 450 RPM, the second stage performance has increased. We also note for the 0.53 kW runner in particular that, apart from the lowest ω, the azimuthal extent of the first and second stages is less than $160°$, which, as noted earlier, is interestingly less than $180°$.

As ω increases above ω_{max}, the difference between β_1 and β_{1b} increases according to Equation (1). The results, documented in [5], indicate that some blades in the first stage eventually produced negative power. This is shown in Figure 7, particularly for $60° \leq \psi \leq 80°$, where β_1 is very high. It is important to note that the behaviour of the runner with negative power has not been recognized before. For $\omega > 450$ RPM, β_1 is too high or the relative velocity W_1 defined in Figure 1 becomes negative and power extraction decreases and becomes negative at small angles. This is the main reason for the runner inefficiency above 450 RPM. At $\omega = 450$ RPM, power production is almost linear in ψ over the entire entry. At lower speeds, $200 < \omega < 300$ RPM, the power extraction increased only slightly toward the right nozzle lip for $80° \leq \psi \leq 130°$. At very high runner speeds, say above $\omega = 450$ RPM, the power production has sharply increased in the azimuthal range $80° \leq \psi \leq 130°$, and is increased as ω increases.
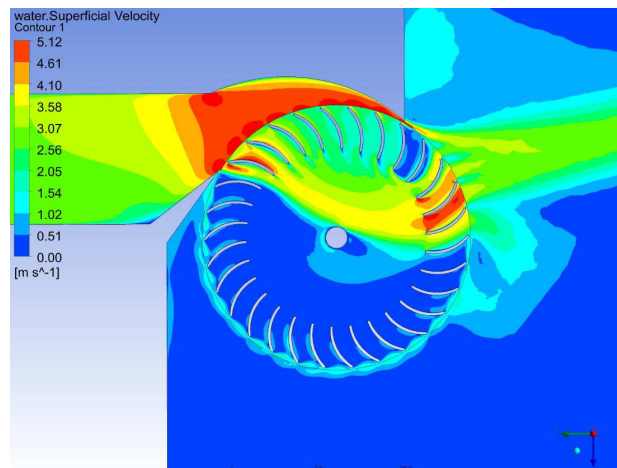
(a)
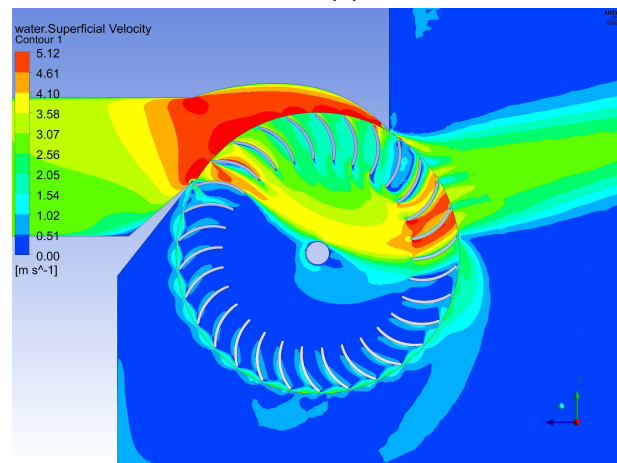
(b)

Figure 6. Contour plot of the magnitude of mean water velocity for the 0.53 kW turbine at maximum efficiency (*H* = 1.337 m, *Q* = 46 lps and *N* = 199.1 RPM). (**a**) the original nozzle with a circular profile; and (**b**) the new nozzle shape given by Equation (3).
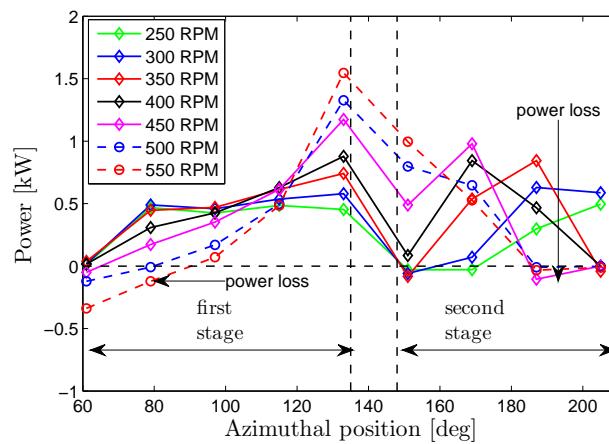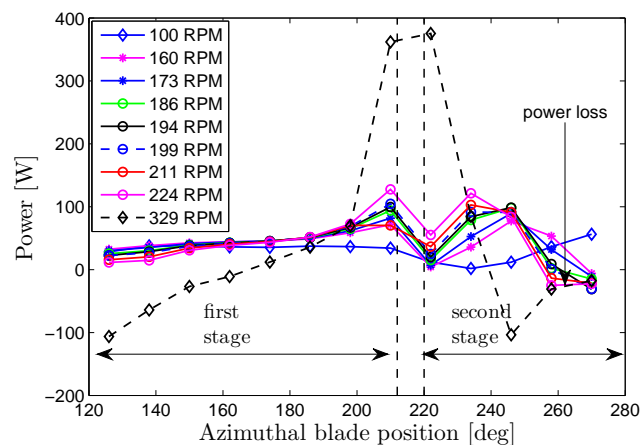

Figure 7. Azimuthal variation of power extraction per blade in the 7 kW turbine at η_{max} and $\omega_{max} = 450$ RPM (*Q* = 105 lps and *H* = 10 m) [5].

The power extraction in the runner of the 0.53 kW turbine, for which $\omega_{max} = 199$ RPM, is shown in Figure 8 for the blades comprising the first and second stages. Both power extraction and β_1 (Figure 19 of [5]) are more uniform in the first stage compared to the 7 kW turbine. A small region of negative power production occurs near the end of the second stage for all ω, due most likely to the variation in β_1. There are differences in the relative power extraction by the first and second stages. At the maximum efficiency, about 69% of the power was extracted at the first stage. This is a remarkable result: very efficient runners can have significant second stage power extraction.

Figure 8. Azimuthal variation of power extraction per blade in the 0.53 kW turbine at η_{max} and $\omega_{max} = 199.1$ RPM ($Q = 46$ lps and $H = 1.337$ m) [5].

3.2. Design Improvement of the 0.53 kW Turbine

Here, we investigate changing the nozzle and runner to improve the turbine efficiency. The detailed computational analysis can be found in [5]. For the design conditions of $Q = 46$ lps and $H = 1.337$ m, which are left unchanged, a range of h_0, θ_s and nozzle width W are possible, but the original choices were assumed to be good and were not changed. They are listed in Table 2. The rear wall shape $R(\theta)$ of the nozzle was redesigned according to [2] as the original nozzle had an arbitrary circular shape. Two nozzle orientations were considered: tangential to the runner at the start of the entry arc and the original nozzle shown in Figure 5. Ref. [2] gives the generalized equation for $R(\theta)$ for non-zero δ shown in Figure 1 as

$$h(\theta_0 + \gamma + \theta) = (\sqrt{(R_1 \sin \theta_0 + h_0)^2 + (R_1 \cos \theta_0)^2} - R_1)(1 - \frac{\theta}{\theta_s - \gamma}), \tag{3}$$

where θ_0 = orientation angle of the left nozzle lip and γ is defined in the Figure. For brevity, the derivation of Equation (3) is omitted here; it can be found in [5]. The original and new nozzle shapes are shown in Figure 9.

The influence of the nozzle designs on the turbine efficiency was small but beneficial. By redesigning the nozzle without altering the runner, η_{max} increased from 88 to 89.45% in the case of original nozzle orientation (vertical). The tangential nozzle gave a very similar efficiency of 89.21%. We provide more significant figures in these η values on the assumption that comparative assessment is likely to be more accurate than absolute assessment. This shows that the orientation of the nozzle has little influence on runner performance. The subsequent redesign of the runner used the original orientation of the nozzle for which Equation (2) gives $\omega_{max} = 183$ RPM, which is slightly lower than the experimentally determined 199 RPM. The new nozzle increased the total entry velocity above that of the original nozzle, showing that more H was converted into kinetic energy and the angular momentum flux at the runner entry. The contours of mean water velocity on the original and new

nozzles are shown in the two parts of Figure 6. It is seen that there is some difference in the water velocities near the rear walls between the two cases.
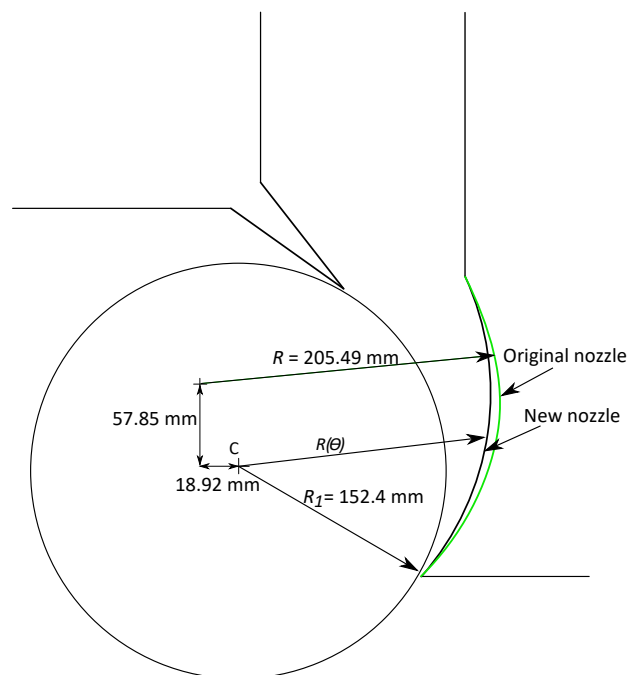

Figure 9. The original and new nozzle design for the 0.53 kW turbine.

Despite the small effect on η, the nozzle orientation has a major influence on β_1. For the tangential nozzle, β_1 is almost uniform at the runner entry and closely matches β_{1b}. As a result, the first stage performance has considerably increased. The percentage power production in the first stage was about 81% at maximum efficiency, whereas, in the original case, it was about 69% [5]. This shows that β_1 directly impacts the relative performance of the two stages and also that the second stage is able to "recover" power "missed" by the first stage.

Subsequent simulations varied R_2/R_1, N_b, β_{1b}, and β_{2b}. A detailed analysis of the influence of these parameters is given by [5]. It was found that all these parameters influence turbine efficiency, of which N_b was the most important. Computations were conducted for $N_b = 20$, 35, and 40. By reducing N_b from the original $N_b = 30$, the first-stage performance decreased accompanied by flow separation on the blades, whereas the second stage performance increased. For example, at $N_b = 20$, η_{max} dropped to 85.87%. By increasing N_b to 35, η_{max} increased to 90%, whereas η_{max} decreased to 88.23% for $N_b = 40$, which is slightly greater than the experimentally determined $\eta_{max} = 86\%$ reported by [20]. At $N_b = 40$, power extraction from both stages decreased. Thus, it was found that the first stage power extraction increased with the increase in N_b only up to the optimum value. The results are summarized in Table 3. Since this study was parametric, no theoretical suggestion for calculating the optimum number of blades has been made. For a Pelton runner, e.g., Zidonis et al. [27], the optimum number of buckets can be estimated using the ratio of water jet diameter and runner diameter. The main design consideration in doing so is to avoid the jet interference with the buckets (due to a high number buckets) as well as the loss of jet (due to a low number of buckets) [27]. This design principle is unlikely to carry over to crossflow turbines because the optimization of N_b is likely to result from a balance between reduction in flow separation and increasing boundary layer blockage as N_b increases. It is highly likely that N_b can be found only by simulation and/or experiment.

Table 3. Influence of blade number on the efficiency of 0.53 kW turbine.

N_b	η_{max} (%)
20	85.87
30	88.45
35	89.87
40	88.23

In summary, we were able to make a modest improvement to the efficiency of this already highly efficient design. The main differences between the original and improved turbine, apart from the nozzle rear wall shape, are listed in Table 2.

3.3. Design Improvement of 7 kW Turbine

The main reason for the lower performance of the 7 kW turbine of [10]—the mismatch of nozzle and runner—was examined in the previous section. To improve the maximum efficiency, the nozzle was first redesigned using the analytical model of [2], and simulations were performed without altering the original runner design [2]. The orientation was kept horizontal as in the original design and the shape was calculated using Equation (3). η_{max} increased from 69 to 87% [2]. This allowed identification of the major changes in the runner entry flow and the runner performance.

For the design Q = 105 lps and H = 10 m, a range of possible values of nozzle throat h_0 and nozzle width W are possible, but those used in the original nozzle design did not allow conversion of H into kinetic energy. Therefore, it was decided to use the same $W/h_0 = 1.14$ as the high efficiency 0.53 kW turbine described above for the redesign of the 7 kW one. For similar reasons, θ_s was increased from 69 to 80°. Then, the principle of converting H into kinetic energy gave $h_0 = 83$ mm and $W = 94.34$ mm, which is significantly smaller than for the original design. We anticipate that a reduced W should reduce manufacturing costs as well as make the turbine more compact.

With the new design, $\beta_1 = 40°$ by Equation (1) and $\eta = \eta_{max}$ at $\omega_{max} = 460$ RPM by Equation (2). A comparison of β_1 and the unchanged $\beta_{1b} = 30°$ for the runner entry from the new nozzle and the original nozzle is shown in Figure 17 of [2]. The difference in optimal speed of 500 RPM for the new nozzle compared to 460 RPM is explained by the fact that β_{1b} has not been reduced from its original value and requires a higher ω to match β_{1b} to β_1. It is noted that there is negligible flow separation in the first stage of the runner compared to the original nozzle as shown in Figure 17 of [2]. There is, however, now some separation on the suction sides of the blades at the second stage. It is also interesting to note that the azimuthal variation of β_1 is very similar to that of the high-efficiency 0.53 kW turbine as discussed in the previous section. This completed the investigation of changes to the nozzle design while keeping the same runner.

With the optimal nozzle design, the runner design was altered to match with the inlet flow. Through a number of simulations by varying β_{1b} and N_b, η_{max} improved to about 91%. Maximum efficiency was achieved for $\beta_{1b} = 39°$ and $N_b = 35$. The parameters of the improved design are provided in Table 2. η_{max} from Equation (2) is unaltered by a change to the runner, but it is noteworthy that the runner redesign has not altered η_{max} from the simulations. For brevity, only the results of the improved nozzle and runner design are presented here. The vectors of the mean of water velocity in the improved design shown in Figure 10 demonstrates fully attached flow in both stages of the runner as compared to a massive flow separation in the original runner with the original nozzle. To better understand the power extraction mechanisms in the new designs, azimuthal variation of power extraction at the first and second stages are plotted in Figure 11. The first stage performance has significantly improved with the new nozzle for the original runner. By increasing the number of blades and the outer blade angle, the first stage performance has further increased. The second stage performance is relatively unchanged in all cases accompanied by a small power loss at the end of the second stage for the most efficient design.
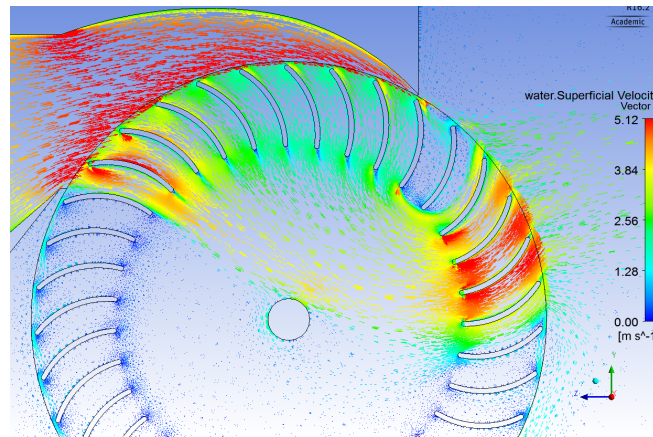
Figure 10. Water velocity vectors illustrating the reduction in flow separation in the runner of the 7 kW turbine with the new nozzle and improved runner design at $\eta_{max} = 91\%$. $Q = 105$ lps, $H = 10$ m, and $N = 500$ RPM. Note that there is a significant reduction in flow separation on the blades [5].
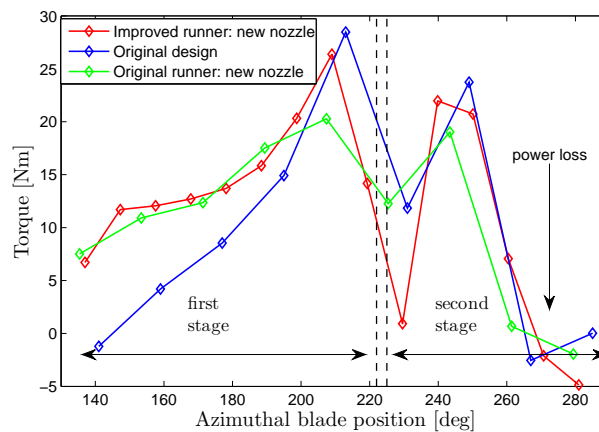

Figure 11. Comparison of torque production in the runner between the improved and the original runner with the new nozzle for the 7 kW turbine at η_{max}. Note that the original runner has $N_b = 20$ and $\beta_{1b} = 30°$, whereas the new runner has $N_b = 35$ and $\beta_{1b} = 39°$. For the purpose of comparison, the data are computed at each blade position and normalized with the torque for 35 blades. The first stage contributions for the original nozzle, the new nozzle with the original runner, and the new nozzle with improved runner are respectively 62%, 69%, and 73% [5].

4. Design Principle for High Efficiency Turbines

The fundamental design principles can now be outlined. It is emphasized that preliminary calculations and reliance on previous parametric studies can only provide an approximate design and do not guarantee high efficiency, so full numerical calculations are recommended in the detailed design followed by turbine testing.

The nozzle should be designed in accordance with the 2D analytical equations given in [2], which include the present Equations (1) and (2). Equation (7) of [2], for example, gives $R(\theta)$ for the general case of non-tangential entry. For the runner design, the following parameters can be recommended based on the design of the most efficient turbines.

- Runner radius ratio: $R_2/R_1 = 0.68$ [5,19]. Table 1 shows little variation in this parameter in experiments and simulations. It is reasonable, however, to assume R_2/R_1 must be sufficiently large to allow the water flow to turn in the air-space before entering the second stage where signifciant power may be extracted. Thus, it is unlikely that R_2/R_1 could be much lower than 0.68.

- Outer and inner blade angles (β_{1b} and β_{2b}, respectively): To minimize flow separation on the blades, β_{1b} should be equal to β_1, which can be computed from Equation (1). For example, $\beta_{1b} \approx 39°$ would be in the maximum efficiency range as obtained by [19] and numerically validated by [5]. Similarly, β_{2b} can be chosen as 90° [5,19]. Since $\beta_{2b} = 55°$ and 90° gave similar efficiencies (about 90% efficiency) in the experiment of [20], this parameter may not be a critical to turbine efficiency.
- Entry arc angle, θ_s, interacts with the runner geometry, Q, and H. $\theta_s = 80°$ to 90° gives the maximum efficiency in the cases considered.
- Nozzle aspect ratio: $W/h_0 = 1.14$ can be a good choice, and was the value for the highest efficiency turbines considered here. In general, W/h_0 probably depends on θ_s and R_1, [5,19]. This parameter determines the width of the runner and nozzle and the overall physical dimensions and weight of the runner.

It is noted that the selection of N_b is critical [5,19,20], and there are no empirical relations or simple theory to guide the choice. For any design, N_b must be optimized using numerical simulations and/or experiments. For preliminary design, $N_b = 30$–35 can be a good choice to be confirmed by detailed simulations. In summary, the choice of the above values of the critical parameters does not guarantee $\eta_{max} \approx 90\%$ but is highly likely to do so.

5. Areas for Research and Development

The literature review revealed few studies of crossflow turbines with high maximum efficiency, η_{max}, so that further experimental and computational studies directed toward turbine designs with $\eta_{max} \approx 90\%$ or above are highly desired. By focusing on the design characteristics of high-efficiency turbines, more efficient turbine designs can be achieved, but it will be a major challenge to exceed 90%. It was found that the crossflow turbine, despite its significant advantages, is the least researched compared to more advanced turbine types such as Pelton and Francis. The following is a list of studies recommended to further improve its design:

- further experimental and numerical studies of turbines with $\eta_{max} \geq 90\%$. Characterization of internal flow features, particularly of the nozzle and assessment of power extracted from the two stages. Measurements of the flow through the blades would be difficult but valuable to check—for example, computational predictions of separation.
- experimental and numerical studies on selection of optimum number of blades. The ratio θ_s/R_1 may be a relevant design parameter when compared to the selection of number of buckets in Pelton runners.
- experimental and numerical studies of dual-nozzle crossflow turbines. The general finding in the simulations that the first and second stages occupy less that 180° suggests this possibility for reducing the size of the runner, improving the power density and runner loading, and reducing vibration.
- experimental and numerical studies on cavitation and its impact on the performance of efficient designs over a wide range of operating conditions. The only investigation to date of cavitation in crossflow turbines was for a low efficiency design.

6. Conclusions

This paper reviews systematically the design methodology for improving the maximum efficiency of crossflow hydroturbines without a guide vane. A standard design can follow the 2D analytical model for the nozzle design reported by [2] and three-dimensional (3D) RANS simulations for evaluating the turbine performance and improving the maximum efficiency as presented in [5].

The review revealed that crossflow turbines can achieve 90% efficiency. A systematic computational study for matching the nozzle and runner designs, which is an important criterion not investigated in detail in the literature, has been performed in [5]. A procedure for designing

optimum nozzles and matching the nozzle and runner designs has been demonstrated through computational study using three-dimensional Reynolds-Averaged Navier–Stokes simulations with an SST k-ω turbulence model and a two-phase homogeneous free-surface flow model. The main conclusions drawn from this review regarding the design of high efficiency crossflow turbines are summarized as follows:

1. The design principle for achieving high efficiency is converting the head at the nozzle inlet into kinetic energy at the runner entry and matching the entry flow with the runner design. A two-dimensional analytical model developed by Adhikari and Wood [2] gives a simple analytic equation for the nozzle rear-wall shape, the condition for converting the head into kinetic energy, and the entry flow angle and the optimum operating speed for the runner design. The usefulness of these results was demonstrated by detailed computational simulations. The simulated runner speed for maximum efficiency was around 6% higher than that from Equation (2) for the highest efficiency designs.

2. Detailed investigation of the power extracted by each blade showed that the relative importance of the first or entry stage could vary significantly without a major impact on turbine performance. The second or exit stage could produce up to 38% of the power. This unique feature of crossflow turbines gives some flexibility in the runner design. For most runners that were studied, the total azimuthal extent of the two stages was less than 180° suggesting that a double nozzle design could further increase the power density and cost effectiveness of crossflow turbines.

Author Contributions: Ram Adhikari and David Wood conceived and designed the literature review and design improvement using RANS simulations. Ram Adhikari performed the flow simulations using high performance computers provided by WestGrid Canada. David Wood and Ram Adhikari synthesized the literature review and analyzed the simulation results. David Wood supervised the research works reported in the paper.

Conflicts of Interest: The authors declare no conflict of interest.

Abbreviations

The following abbreviations are used in this manuscript:

CFD　　　Computational Fluid Dynamics
RANS　　Reynolds-Averaged Navier–Stokes Simulation
3D　　　　Three-dimensional

References

1. Michell, A. Impulse-Turbine. U.S. Patent 760,898, 24 May 1904.
2. Adhikari, R.; Wood, D. A new nozzle design methodology for high efficiency crossflow hydro turbines. *Energy Sustain. Dev.* **2017**, *41*, 139–148.
3. Paish, O. Small hydro power: Technology and current status. *Renew. Sustain. Energy Rev.* **2002**, *6*, 537–556.
4. Sinagra, M.; Sammartano, V.; Aricò, C.; Collura, A.; Tucciarelli, T. Cross-Flow turbine design for variable operating conditions. *Procedia Eng.* **2014**, *70*, 1539–1548.
5. Adhikari, R. Design Improvement of Crossflow Hydro Turbine. Ph.D. Thesis, University of Calgary, Calgary, AB, Canada, 2016.
6. Choi, Y.D.; Lim, J.I.; Kim, Y.T.; Lee, Y.H. Performance and internal flow characteristics of a cross-flow hydro turbine by the shapes of nozzle and runner blade. *J. Fluid Sci. Technol.* **2008**, *3*, 398–409.
7. Macmore, C.; Merryfield, F. *The Banki Water Turbine*; Engineering Experiment Station: College Station, TX, USA, 1949.
8. Varga, J. Tests with the Banki water turbine. *Acta Tech. Acad. Hung.* **1959**, 26, 79–102.
9. Durali, M. Design of Small Water Turbines for Farms and Small Communities. Ph.D. Thesis, Massachusetts Institute of Technology, Cambridge, MA, USA, 1976.

10. Dakers, A.; Martin, G. Development of a Simple Cross-flow Water Turbine for Rural Use. In *Agricultural Engineering Conference 1982: Resources, Efficient Use and Conservation*; Preprints of Papers; Institution of Engineers, Canberra, Australia, 1982; p. 35.

11. Johnson, W.; White, E.R.; White, F. Design and testing of an inexpensive crossflow turbine. In *Small Hydropower Fluid Machinery*; ASME: New York, NY, USA, 1982.

12. Nakase, Y.; Fukutomi, J.; Watanabe, T.; Suetsugu, T.; Kubota, T.; Kushimoto, S. A study of Cross-Flow turbine (Effects of nozzle shape on its performance). In Proceedings of the Winter Annual Meeting ASME, Phoenix, AZ, USA, 14–19 November 1982; Volume 1419.

13. Durgin, W.; Fay, W. Some fluid flow characteristics of a cross-flow type hydraulic turbine. In *Small Hydro Power Fluid Machinery*; ASME: New York, NY, USA, 1984; pp. 77–83.

14. Khosrowpanah, S. Experimental Study of the Crossflow Turbine. Ph.D. Thesis, Colorado State University, Fort Collins, CO, USA, 1984.

15. Khosrowpanah, S.; Fiuzat, A.; Albertson, M.L. Experimental study of crossflow turbine. *J. Hydraul. Eng.* **1988**, *114*, 299–314.

16. Hothersall, R. A review of the cross-flow turbine. In *Waterpower '85, Proceedings of the International Conference on Hydropower, Las Vegas, NV, USA, 25–27 September 1985*; ASCE: New York, NY, USA, 1985.

17. Ott, R.F.; Chappell, J.R. Design and efficiency testing of a cross-flow turbine. In *Waterpower'89, Proceedings of the International Conference on Hydropower, Niagara Falls, NY, USA, 23–25 August 1989*; ASCE: New York, NY, USA, 1989; pp. 1534–1543.

18. Fiuzat, A.; Akerkar, B. The Use of Interior Guide Tube in Cross Flow Turbines. In *Waterpower'89, Proceedings of the International Conference on Hydropower, Niagara Falls, NY, USA, 23–25 August 1989*; American Society of Civil Engineers: New York, NY, USA, 1989; pp. 1111–1119.

19. Desai, V.R. A Parametric Study of the Cross-flow Turbine Performance. Ph.D. Thesis, Clemson University, Clemson, SC, USA, 1993.

20. Totapally, H.G.; Aziz, N.M. Refinement of Cross-flow Turbine Design Parameters. *J. Energy Eng.* **1994**, *120*, 133–147.

21. Adhikari, R.C.; Vaz, J.; Wood, D. Cavitation Inception in Crossflow Hydro Turbines. *Energies* **2016**, *9*, 237.

22. Fiuzat, A.A.; Akerkar, B.P. Power outputs of two stages of cross-flow turbine. *J. Energy Eng.* **1991**, *117*, 57–70.

23. De Andrade, J.; Curiel, C.; Kenyery, F.; Aguillón, O.; Vásquez, A.; Asuaje, M. Numerical investigation of the internal flow in a Banki turbine. *Int. J. Rotating Mach.* **2011**, *2011*, 841214.

24. Sammartano, V.; Aricò, C.; Carravetta, A.; Fecarotta, O.; Tucciarelli, T. Banki-Michell optimal design by computational fluid dynamics testing and hydrodynamic analysis. *Energies* **2013**, *6*, 2362–2385.

25. Acharya, N.; Kim, C.G.; Thapa, B.; Lee, Y.H. Numerical analysis and performance enhancement of a cross-flow hydro turbine. *Renew. Energy* **2015**, *80*, 819–826.

26. Sammartano, V.; Morreale, G.; Sinagra, M.; Tucciarelli, T. Numerical and experimental investigation of a cross-flow water turbine. *J. Hydraul. Res.* **2016**, *54*, 321–331.

27. Židonis, A.; Aggidis, G.A. Pelton turbine: Identifying the optimum number of buckets using CFD. *J. Hydrodyn. Ser. B* **2016**, *28*, 75–83.